Variational Frameworks for DT-MRI Estimation, Regularization and Visualization

David Tschumperlé　　Rachid Deriche

Odyssée Lab, INRIA Sophia-Antipolis
2004 Rte des Lucioles, BP 93
06902 Sophia-Antipolis, France

Abstract

We address three crucial issues encountered in DT-MRI (Diffusion Tensor Magnetic Resonance Imaging) : diffusion tensor Estimation, Regularization and fiber bundle Visualization. We first review related algorithms existing in the literature and propose then alternative variational formalisms that lead to new and improved schemes, thanks to the preservation of important tensor constraints (positivity, symmetry). We illustrate how our complete DT-MRI processing pipeline can be successfully used to construct and draw fiber bundles in the white matter of the brain, from a set of noisy raw MRI images.

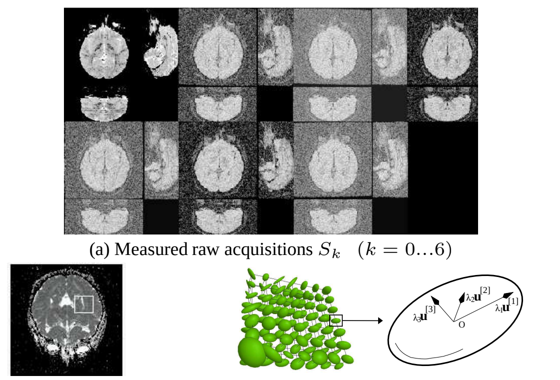

(a) Measured raw acquisitions S_k $(k = 0...6)$

(b1) Mean diffusivity = $\frac{1}{3}(\lambda_1 + \lambda_2 + \lambda_3)$

(b2) Part of the tensor field, represented with 3D ellipsoids.

Figure 1. Principle of DT-MRI Imaging

1. Introduction

The recent introduction of DT-MRI (Diffusion Tensor Magnetic Resonance Imaging) has raised a strong interest in the medical imaging community [3, 15]. This non-invasive 3D modality consists in measuring the water molecule motion within the tissues, using magnetic resonance techniques. Basically, it is based on the rendering of multiple raw MRI images $S_k : \Omega \subset \mathbb{R}^3 \rightarrow \mathbb{R}$ using pulse sequences based on several gradient directions and magnitudes (at least 6 noncolinear directions are needed). Moreover, an additional image S_0 is measured without preferred gradient direction (Fig.1a). Note that these S_k may be quite noisy, due to the high speed needed for these multiple MRI acquisitions. This large set $\{S_k, k = 0...n\}$ of raw data is then estimated into a corresponding volume $\mathbf{T} : \Omega \subset \mathbb{R}^3 \rightarrow \mathrm{P}(3)$ of Diffusion Tensors (i.e 3x3 symmetric and positive-definite matrices) that describe through their spectral elements, the main diffusivities $\lambda_1, \lambda_2, \lambda_3$ (with $\lambda_1 \geq \lambda_2 \geq \lambda_3$) and the corresponding orthogonal directions $\mathbf{u}$,$\mathbf{v}$,$\mathbf{w}$ of the water molecule diffusion process in tissues such as bones, muscles and white matter of the brain (Fig.1b). $\forall x, y, z \in \Omega, \quad \mathbf{T}(x, y, z) = \lambda_1 \mathbf{u}\mathbf{u}^T + \lambda_2 \mathbf{v}\mathbf{v}^T + \lambda_3 \mathbf{w}\mathbf{w}^T$. Depending on the characteristics of the tissue, the diffusion (and then the estimated tensors) can be isotropic, for instance in the areas with fluids such in the CSF filled ventricles, or anisotropic as in the white matter of the brain where the diffusion is mainly performed in the direction of the neuron fibers [16, 37, 38]. DT-MRI is then particularly well adapted to study the neuron connectivities within white matter, by tracking the fiber directions given pointwise by the principal eigenvector $\mathbf{u}(x, y, z)$ of the tensor $\mathbf{T}(x, y, z)$.

Actually, retrieving the fiber bundles from the raw images S_k involves a lot of subjacent processes : First the *estimation part* that computes the tensor field $\mathbf{T}$ from the set of raw MRI volumes S_k. As the estimation result may be noisy, a *tensor field regularization process* can be necessary. Finally, fibers must be tracked and *visualized*, in a practical and understandable way. In this paper, we propose a survey of existing methods trying to solve these issues and we introduce new variational frameworks that take important tensor structural constraints into account, resulting in improved algorithms for these three decisive steps in DT-MRI. We finally illustrate how our stand-alone set of approaches can be used as a pipeline to obtain fiber tracking results from synthetic and real raw MRI datasets of the brain.

2. Estimation of Diffusion Tensors

2.1. Review of existing methods

Estimating a field of 3×3 diffusion tensors (symmetric and positive-definite matrices) from a set of raw MRI images $S_k : \Omega \rightarrow \mathbb{R}$ is usually done by solving for each voxel the Stejskal-Tanner equation [24] :

$$\forall (x,y,z) \in \Omega, \quad S_{k_{(x,y,z)}} = S_{0_{(x,y,z)}} \; e^{-g_k^T \mathbf{T}_{(x,y,z)} g_k} \quad (1)$$

where $g_k \in \mathbb{R}^3$ is the vector whose coordinates represent the pulse gradient direction/magnitude, used for the acquisition of the volume S_k. Classical methods for computing the tensor $\mathbf{T}$ from the images S_k are as follows :

• **Direct tensor estimation :** Authors in [36, 38] proposed an elegant closed-form to estimate the tensors $\mathbf{T}$ directly from a set of 7 raw images. Their method is based on the decomposition of $\mathbf{T}$ into a specific orthonormal tensor basis $\tilde{g_k}\tilde{g_k}^T$ computed as the dual basis of $\{ \; g_k g_k^T \mid k = 1..6 \; \}$, the original basis used for the measurement of the S_k :

$$\mathbf{T} = \sum_{k=1}^{6} \ln\left(\frac{S_0}{S_k}\right) \tilde{g_k}\tilde{g_k}^T \quad (2)$$

Unfortunately, only 7 images $S_0, ..., S_6$ can be used to estimate the tensor field $\mathbf{T}$. As illustrated in Fig.2c, this low number of images may be not sufficient for a robust estimation of $\mathbf{T}$ especially if the S_k are corrupted with noise.

• **Least square estimation (LS)** : It is the most classical method used for diffusion tensor computation [2, 20]. The tensors $\mathbf{T}$ are estimated by solving the following least square criterion,

$$\min_{\mathbf{T} \in \mathcal{M}_3} \quad \sum_{k=1}^{n} \left(\ln\left(\frac{S_0}{S_k}\right) - g_k^T \mathbf{T} g_k \right)^2 \quad (3)$$

which leads to the resolution of an overconstrained system $\mathbf{A}\mathbf{x} = \boldsymbol{\mathcal{B}}$ (where $\mathbf{x}$ is a vector containing the six unknown coefficients of $\mathbf{T}$). The LS method is more robust, since all the n available raw images S_k (usually $n > 7$) are used for the tensor estimation.

Note that both methods do not take the prior positive-definiteness constraint of the tensors $\mathbf{T}$ into account. For the case of noisy raw images, nothing prevents the estimation process to compute *negative tensors*. Practically, one solution could be to reproject the negative tensors into the positive tensor space after such estimation method. This is generally done by forcing negative eigenvalues of the tensors to zero. Note also that both estimation processes are purely *pointwise* : no spatial interactions between tensors are considered.

2.2. A variational approach

We propose to avoid these important drawbacks by using a variational approach that estimates the tensor field $\mathbf{T}$ while introducing important priors on the *tensor positivity* and *regularity*. Our idea is based on the *positive-constrained minimization* of the following functional :

$$\min_{\mathbf{T} \in \mathrm{P}(3)} \int_\Omega \sum_{k=1}^{n} \psi\left(\left| \ln\left(\frac{S_0}{S_k}\right) - g_k^T \mathbf{T} g_k \right| \right) + \alpha \, \phi(\|\nabla \mathbf{T}\|) \; d\Omega \quad (4)$$

where $\psi : \mathbb{R} \rightarrow \mathbb{R}$ is a function allowing a robust tensor estimation, $\phi : \mathbb{R} \rightarrow \mathbb{R}$ is an increasing function acting as an anisotropic regularizer of the tensor field, $\alpha \in \mathbb{R}$ is a user-defined regularization weight and $\|\nabla \mathbf{T}\| = \left(\sum_{i,j} \|\nabla T_{i,j}\|^2\right)^{\frac{1}{2}}$ stands for the classical Frobenius matrix norm. Note that if $\psi(s) = s^2$ and $\alpha = 0$, we minimize the LS criterion (3), but with a positive solution since our minimization is done on *the constrained space* $\mathrm{P}(3)$ *of the positive tensors*. Following our previous works in [9, 27], the gradient descent (PDE) that minimizes (4) in $\mathrm{P}(3)$ is :

$$\begin{cases} \mathbf{T}_{(t=0)} = \mathbf{Id} & \textit{(}3 \times 3 \textit{ identity matrices)} \\ \frac{\partial \mathbf{T}}{\partial t} = (\mathbf{G} + \mathbf{G}^T)\mathbf{T}^2 + \mathbf{T}^2(\mathbf{G} + \mathbf{G}^T) \end{cases} \quad (5)$$

where $\mathbf{G}$ corresponds to the unconstrained velocity matrix defined as : $G_{i,j} = \sum_{k=1}^{n} \psi^{'}(|v_k|)\mathrm{sign}(v_k) \left(g_k g_k^T\right)_{i,j} + \alpha \mathrm{div}\left(\frac{\phi^{'}(\|\nabla \mathbf{T}\|)}{\|\nabla \mathbf{T}\|} \; \nabla T_{i,j} \right)$, with $v_k = \ln\left(\frac{S_0}{S_k}\right) - g_k^T \mathbf{T} g_k$.

Eq.(5) ensures the *positive-definiteness* of the tensors $\mathbf{T}$ for each iteration of the estimation process. Moreover, the regularization term α introduces *spatial regularity* on the estimating tensor field, while preserving important physiological discontinuities, thanks to the anisotropic behavior of the ϕ-function regularization formulation (as described in the broad literature on anisotropic smoothing with PDE's, see [1, 23, 26, 34] and references therein). Concerning the implementation part, a specific reprojection-free numerical scheme based on matrix exponentials can be used for this PDE flow (5) (see [9, 10] for more details) :

$$\mathbf{T}_{(t+dt)} = \mathbf{A}^T \mathbf{T}_{(t)} \mathbf{A} \;\; \text{with} \;\; \mathbf{A} = \exp\left(\mathbf{T}_{(t)}(\mathbf{G} + \mathbf{G}^T)dt\right)$$

Our iterative method starts then from a field of isotropic tensors that are evolving in $\mathrm{P}(3)$ and are morphing until their shapes fit the measured data S_k. The respect of the positiveness and regularity constraints has a large interest for DT-MRI estimation, and leads to more accurate results than with classical methods (illustration on Fig.2c,d,e, with the estimation of a synthetic field). For our experiments, we chose $\psi(s) = \log(1 + s^2)$ ("Lorentzian" function), and $\phi(s) = \sqrt{1 + s^2}$ ("Hypersurface" function, [8]) which gave the best estimation results. Note that very recently, a similar variational approach for tensor estimation has been proposed [32]. But the proposed method doesn't deal with various estimator and regularizer functionals and doesn't estimates the tensors in the constrained space $\mathrm{P}(3)$, leading to the possible computation of negative tensors.

3. DT-MRI Regularization

The regularization term in eq.(5) acts as a matrix spatial regularizer. After the estimation process, it can be interesting to regularize more precisely the tensor field and more particularly its spectral features. Indeed they are the relevant informations (diffusivities and tensor orientations) used for the fiber tracking and for the computation of interesting physiological indices such as the mean diffusivity $\tilde{\lambda} = \frac{1}{3}(\lambda_1 + \lambda_2 + \lambda_3)$ or the Fractional Anisotropy $FA = (\frac{3}{2} \; \frac{(\lambda_1-\tilde{\lambda})^2+(\lambda_2-\tilde{\lambda})^2+(\lambda_3-\tilde{\lambda})^2}{\lambda_1^2+\lambda_2^2+\lambda_3^2})^{\frac{1}{2}}$ that characterizes different biological tissues. Regularizing a DT-MRI volume helps then for the retrieval of more coherent tensor structural informations.

3.1. Review of existing methods

The problem of DT-MRI regularization/denoising with PDE's has been recently tackled in the literature. Proposed algorithms can be grouped in two classes :

• **Non-spectral methods** are either based on a direct anisotropic smoothing of the raw image data S_k [31], or directly the 3×3 matrix field describing the estimated tensors [35], while taking eventual coupling between these multi-valued components into account. Such methods have to be applied carefully : Tensor diffusivities and orientations are regularized at the same time, and diffusivities may be regularized more fastly than tensor orientations, leading to an *eigenvalues swelling effect*, as described in [27].

• **Spectral methods** are based on the separate regularization of the tensor eigenvalues and eigenvectors. The field of diffusivities $\Omega \rightarrow (\lambda_1, \lambda_2, \lambda_3)$ may be considered as a vector-valued image, and treated with one of the numerous existing regularization PDE's, preserving the positivity of the values (see [14, 23, 26, 29, 34] and references therein). The regularization of the tensor orientations is more arduous, since it must act on three orthonormal eigenvectors (or equivalently on orthogonal 3×3 matrices). In [13, 27], the authors proposed PDE's acting either on the principal eigenvector $\mathbf{u}$ (then a tensor reconstruction is needed), or directly on the field of orthogonal matrices $\mathbf{R} = (\mathbf{u}|\mathbf{v}|\mathbf{w})$ corresponding to the tensor orientations. In both cases, proposed methods suffer from the problem of *eigenvector realignment* : a spectral decomposition of a tensor field $\mathbf{T}$ is not unique and can give discontinuous orientation fields $\mathbf{u}, \mathbf{v}, \mathbf{w}$, even if $\mathbf{T}$ is perfectly continuous. This requires then time-consuming realignement for each PDE iteration.

3.2. A fast spectral method

Following our previous work in [9], we propose a simple way to avoid this eigenvector discontinuity problem. Our alternative approach is based on the fact that restoring tensor orientations do not necessarily need the computation of the eigenvectors. The idea lies on the use of an *isospectral flow*, that regularizes the tensor field *while preserving the eigenvalues of the considered tensors*. As a result, only tensor orientations are regularized. As we measure directly the tensor field variations from the gradients of the matrix coefficients, no false discontinuities have to be managed. The general form of an isospectral flow is (see [9, 11, 12]) :

$$\frac{\partial \mathbf{T}}{\partial t} = [\mathbf{T}, [\mathbf{T}, (\mathbf{G}+\mathbf{G}^T)]] \;\; \text{with} \;\; [\mathbf{A}, \mathbf{X}] = \mathbf{AX} - \mathbf{XA} \quad (6)$$

Here, we choose the matrix-valued term $\mathbf{G}$ to correspond to the desired regularization process : $\mathbf{G} = (G_{i,j})$ with $G_{i,j} = \mathrm{div}\left(\frac{\phi'(\|\nabla \mathbf{T}\|)}{\|\nabla \mathbf{T}\|} \nabla T_{i,j}\right)$, where $\phi(s) = \sqrt{1+s^2}$ is a classical ϕ-function leading to discontinuity-preserving regularization [8]. Note that other regularization terms $\mathbf{G}$ may be suitable, as those proposed in [14, 23, 26, 29, 34]. Indeed, Eq.(6) is a really general formalism to work only *on diffusion tensor orientations*. A specific reprojection-free scheme based on matrix exponentials can be also used to implement the isospectral PDE (6) :

$$\mathbf{T}_{(t+dt)} = \mathbf{A}^T \mathbf{T}_{(t)} \mathbf{A} \;\; \text{with} \;\; \mathbf{A} = \exp\left(dt[\mathbf{G} + \mathbf{G}^T, \mathbf{T}_{(t)}]\right)$$

The use of two regularization processes (one for the tensor diffusivities, and one for the tensor orientations) allows us to get a better regularization control on the important structural informations of the tensors. This is a natural complement to the simpler regularization technique used in our estimation method (4).

4. Fiber Visualization

DT-MRI images are well suited to study the fiber network in the white matter of the brain. The need to visualize such fibers bundles has recently raised a strong interest for specific visualization techniques dedicated to this issue. Common visualization methods used with DT-MRI images are :

• **Ellipsoids** are the natural representations of diffusion tensors. They are well adapted to see independently each DT-MRI voxel, and its spectral elements. Nevertheless, they are not suitable to display large fields because of the high number of ellipsoids needed : as illustrated on Fig.2m (left), displays of large fields with ellipsoids can be confusing.

• **Streamlines** are parametric representations of the fibers. They are constructed from the tensor field by drawing lines following the diffusion tensor principal orientations $\mathbf{u}$. Well adapted for displaying fibers of medium-size parts of the tensor field, they can also be confusing for larger ranges of view (Fig.2m (right)).

• **LIC** (line integral convolution). As proposed in [6, 17], the idea is to integrate a noise texture in the direction of the principal tensor direction, leading to a texture-representation of the flow. It is more adapted to display fibers in larger DT-MRI regions, but is a time-consuming process.

We propose here an alternative method to the LIC, based on regularization PDE's. The idea is as follows. We first compute a noisy 3D volume $I_0 : \tilde{\Omega} \rightarrow \mathbb{R}$ where $\tilde{\Omega}$ designates a scaled version of the original DT-MRI domain Ω. Then, we apply this specific PDE flow :

$$\frac{\partial I}{\partial t} = \mathrm{trace}\,(\mathbf{DH}) \tag{7}$$

where $\mathbf{D} : \Omega \rightarrow \mathrm{P}(3)$ is a diffusion tensor field computed as $\mathbf{D} = \mathbf{u}\mathbf{u}^T + g(FA)\;(\mathbf{Id} - \mathbf{u}\mathbf{u}^T)$, where $\mathbf{u}$ is the principal direction of $\mathbf{T}$, $\mathbf{Id}$ is the 3×3 identity matrix and $g : [0,1] \rightarrow [0,1]$ is a decreasing function. This equation (7) has the interesting property of smoothing the image I in the principal directions of the tensors where they are anisotropic (i.e. $FA(x,y,z) >> 0$), while performing an isotropic smoothing where tensors are isotropic (i.e. $FA(x,y,z) \simeq 0$). Recently in [26, 30], we proved that this trace-based equation has an interpretation in terms of local smoothing, which is not always the case for equivalent divergence-based operators (as the one recently proposed in [5, 22]). The PDE (7) constructs iteratively a scale-space textured representation of the fibers and has to be stopped after a finite number of iterations. Then, we can multiply the pixels of the obtained image by the Fractional Anisotropy FA in order to highlight the regions of high density fibers (as done on Fig.2n,o, at two different scales).

5. Applications

We applied our three proposed algorithms for DT-MRI processing with synthetic and real data (of the white matter of the brain). Our real dataset is composed of 31 images with a resolution of $128 \times 128 \times 56$, corresponding to raw measurements in 6 gradient directions, each with 5 increasing magnitudes (courtesy of CEA-SHFJ/Orsay, France) [1] . Results are illustrated on Fig.2.

• **Tensor Estimation** : From a synthetic tensor field (Fig.2b), we generated its corresponding raw MRI measures (31 images), that we corrupted with gaussian noise (Fig.2a shows a subset of 6 of these raw images). We illustrate the results obtained with the three different estimation methods presented in this paper. It is clear that our variational method is more robust to the noise, thanks to the respect of the prior positivity constraint, as well as the use of a spatial regularizer during the tensor estimation.

• **Regularization** : The regularization of diffusion tensors fields is illustrated with a synthetic and real case. The effect of our isospectral flow is showed on Fig.2f,g,h. Despite the high orientation noise that has been added to the synthetic tensor field, no eigenvalue swelling effect appear, since we act only on the orientation part. We also have a fine control on the diffusivity part (Fig.2i,j), that allows us to compute for instance denoised fractional anisotropy FA. A detail of the corpus callosum is presented in Fig.2k,l. Note that with the regularized field, we retrieve much more coherent fiber networks.

• **Visualization** : As explained in section 4, our PDE-based technique is usefull to generate large representation of fiber bundles. The directions of the fibers are clearly visible in the create texture image, whereas the parametric representation for the same region is more confusing. (Fig.2m,n,o).

[1]The authors would like to thank J-F Mangin and J-B Poline for providing us with the data, as well as C. Chefd'hotel for our previous collaborations that inspired the algorithms proposed in this paper.

6. Conclusion

We proposed a complete set of DT-MRI processing tools that proposes alternative formulations to classical algorithms encountered in important issues of DT-MRI imaging : We introduced the positive-definiteness constraint for the tensor estimation part and we proposed specific regularization methods, respecting the important spectral features of the tensors. Both processes use adapted numerical schemes avoiding any constraint-preservation problems and speeding up the computation. Finally, texture-based generation of the fibers has been proposed, allowing to visualize easily DT-MRI fiber networks at multiple scales.

References

[1] L. Alvarez, P.L. Lions, and J.M. Morel. Image selective smoothing and edge detection by nonlinear diffusion (II). *SIAM Journal of Numerical Analysis*, 29:845–866, 1992.

[2] P.J. Basser, J. Mattiello, and D. LeBihan. Estimation of the effective self-diffusion tensor from the NMR spin echo. *Journal of Magnetic Resonance*, B(103):247–254, 1994.

[3] P.j. Basser, J. Mattiello, and D. LeBihan. MR diffusion tensor spectroscopy and imaging. *Biophysica*, (66):259–267, 1994.

[4] P.J. Basser and S. Pajevic. Statistical artifacts in diffusion tensor MRI caused by background noise. *Magnetic Resonance in Medicine*, 44:41–50, 2000.

[5] J. Becker, T. Preusser, and M. Rumpf. Pde methods in fbw simulation post processing. *Computing and Visualization in Science*, 3(3):159–167, 2000.

[6] B. Cabral. Imaging vector fi elds using line integral convolution. In *Computer Graphics Proceedings*, pages 263–270, 1993.

[7] J.S.W. Campbell, K. Siddiqi, B.C. Vemuri, and G.B Pike. A geometric fbw for white matter fi bre tract reconstruction. In *IEEE International Symposium on Biomedical Imaging Conference Proceedings*, pages 505–508, July 2002.

[8] P. Charbonnier, G. Aubert, M. Blanc-Féraud, and M. Barlaud. Two deterministic half-quadratic regularization algorithms for computed imaging. In *Proceedings of the International Conference on Image Processing*, volume II, pages 168–172, 1994.

[9] C. Chefd'hotel, D. Tschumperlé, R. Deriche, and O. Faugeras. Constrained fbws on matrix-valued functions :

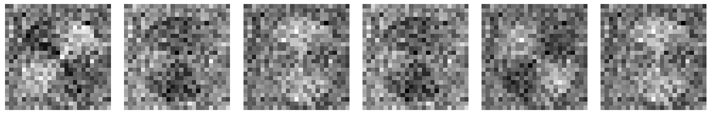

(a) Partial set of noisy raw images S_k (in 6 different gradient directions)

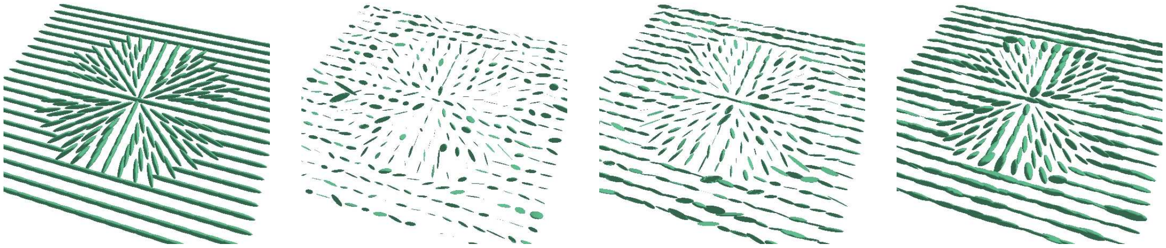

(b) Corresponding true tensor field

(c) Direct estimation with 7 non-colinear images [36].

(d) Least square estimation

(e) Our variational method eq.(5), using positivity and regularity constraints

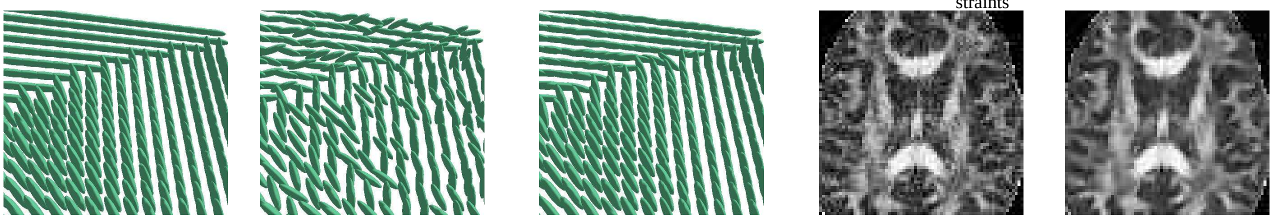

(f) Synthetic tensor field

(g) Adding orientation noise

(h) Result of our isospectral flow (6)

(i) Original FA

(j) Regularized FA, using [30]

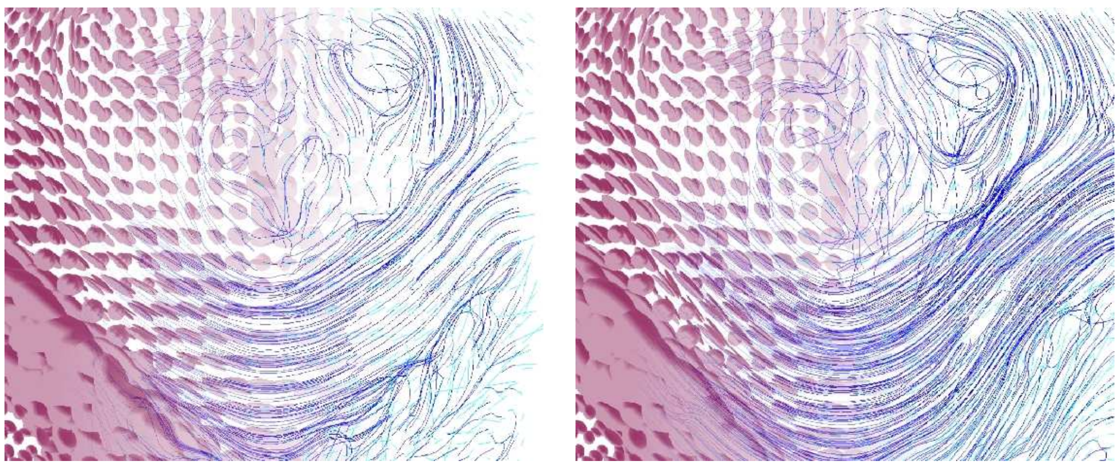

(k) Part of the Corpus Callosum, before tensor field regularization

(l) After tensor field regularization, using (6) and [30].

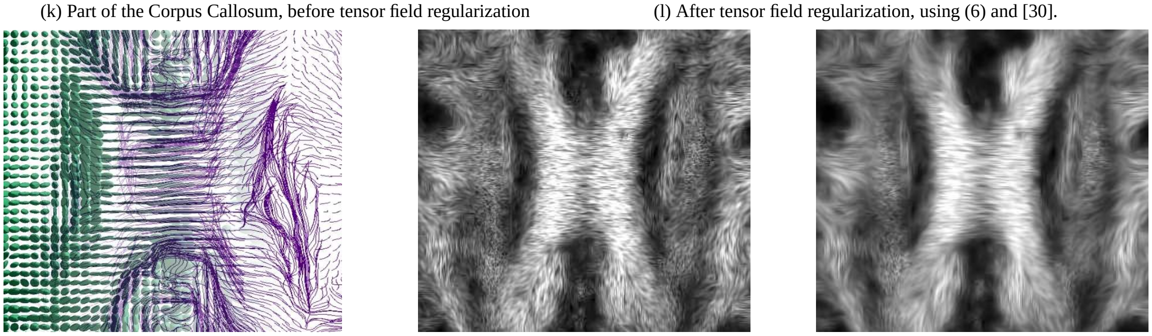

(m) Tensor field displayed with ellipsoids (left) and parametric tracked fibers (right)

(n) Display using our PDE approach (7) (10 iter.)

(o) Display using our PDE approach (7) (30 iter.)

Figure 2. DT-MRI Processing : Estimation (a,b,c,d), Regularization (e,f,g,h,i,j,k,l) and Visualization (m,n,o)

application to diffusion tensor regularization. In *Proceedings of ECCV'02*, June 2002.

[10] C. Chefd'hotel, D. Tschumperlé, R. Deriche, and O. Faugeras. Regularizing flows for constrained matrix-valued images. *Journal of Mathematical Imaging and Vision (JMIV, to appear)*, 2003.

[11] M.T. Chu. Constructing symmetric nonnegative matrices with prescribed eigenvalues by differential equations. Technical report, Department of Mathematics, North Carolina State University, August 1990.

[12] M.T. Chu. A list of matrix flows with applications. Technical report, Department of Mathematics, North Carolina State University, 1990.

[13] O. Coulon, D.C. Alexander, and S.R. Arridge. A regularization scheme for diffusion tensor magnetic resonance images. In *XVIIth International Conferenceon Information Processing in Medical Imaging*, 2001.

[14] R. Kimmel, R. Malladi, and N. Sochen. Images as embedded maps and minimal surfaces: movies, color, texture, and volumetric medical images. *International Journal of Computer Vision*, 39(2):111–129, September 2000.

[15] D. Le Bihan. Methods and applications of diffusion MRI. In I.R. Young, editor, *Magnetic Resonance Imaging and Spectroscopy in Medicine and Biology*. John Wiley and Sons, 2000.

[16] H. Mamata, Y. Mamata, C.F. Westin, M.E. Shenton, F.A. Jolesz, and S.E. Maier. High-resolution line-scan diffusion-tensor MRI of white matter fiber tract anatomy. In *In AJNR Am NeuroRadiology*, volume 23, pages 67–75, 2002.

[17] T.E. McGraw. Neuronal fiber tracking in DTMRI. Master's thesis, University of Florida, 2002.

[18] P. Perona. Orientation diffusions. *IEEE Transactions on Image Processing*, 7(3):457–467, March 1998.

[19] P. Perona and J. Malik. Scale-space and edge detection using anisotropic diffusion. *IEEE Transactions on Pattern Analysis and Machine Intelligence*, 12(7):629–639, July 1990.

[20] C. Poupon. *Détection des faisceaux de fibres de la substance blanche pour l'étude de la connectivité anatomique cérébrale.* PhD thesis, Ecole Nationale Supérieure des Télécommunications, December 1999.

[21] C. Poupon, J.F Mangin, V. Frouin, J. Regis, F. Poupon, M. Pachot-Clouard, D. Le Bihan, and I. Bloch. Regularization of MR diffusion tensor maps for tracking brain white matter bundles. In Proceedings of *MICCAI'98*, vol. 1496, LNCS, pages 489–498, Cambridge, MA, USA, October 1998. Springer.

[22] T. Preusser and M. Rumpf. Anisotropic nonlinear diffusion in flow visualization. In *In Proceedings IEEE Visualization '01*, 2001.

[23] G. Sapiro. *Geometric Partial Differential Equations and Image Analysis*. Cambridge University Press, 2001.

[24] E.O. Stejskal and J.E. Tanner. Spin diffusion measurements: spin echoes in the presence of a time-dependent field gradient. *Journal of Chemical Physics*, 42:288–292, 1965.

[25] B. Tang, G. Sapiro, and V. Caselles. Diffusion of general data on non-flat manifolds via harmonic maps theory : The direction diffusion case. *The International Journal of Computer Vision*, 36(2):149–161, February 2000.

[26] D. Tschumperlé. *PDE's Based Regularization of Multivalued Images and Applications*. PhD thesis, Université de Nice-Sophia Antipolis, December 2002.

[27] D. Tschumperlé and R. Deriche. Diffusion tensor regularization with constraints preservation. In *IEEE Computer Society Conference on Computer Vision and Pattern Recognition*, Kauai Marriott, Hawaii, December 2001.

[28] D. Tschumperlé and R. Deriche. Regularization of orthonormal vector sets using coupled PDE's. In *IEEE Workshop on Variational and Level Set Methods*, pages 3–10, Vancouver, Canada, July 2001.

[29] D. Tschumperlé and R. Deriche. Diffusion PDE's on Vector-Valued images. *IEEE Signal Processing Magazine*, 19(5):16–25, 2002.

[30] D. Tschumperlé and R. Deriche. Vector-valued image regularization with PDE's : A common framework for different applications. In *IEEE Conference on Computer Vision and Pattern Recognition* Madison, Wisconsin (United States), June 2003.

[31] B. Vemuri, Y. Chen, M. Rao, T. McGraw, T. Mareci, and Z. Wang. Fiber tract mapping from diffusion tensor MRI. In *1st IEEE Workshop on Variational and Level Set Methods in Computer Vision (VLSM'01)*, July 2001.

[32] Z. Wang, B.C. Vemuri, Y. Chen, and T. Mareci. Simultaneous smoothing and estimation of the tensor field from diffusion tensor MRI. In *IEEE Conference on Computer Vision and Pattern Recognition* pages 461–466. Madison, Wisconsin (United States), June 2003.

[33] J. Weickert. Coherence-enhancing diffusion of colour images. *7th National Symposium on Pattern Recognition and Image Analysis*, April 1997.

[34] J. Weickert. *Anisotropic Diffusion in Image Processing*. Teubner-Verlag, Stuttgart, 1998.

[35] J. Weickert and T. Brox. Diffusion and regularization of vector and matrix-valued images. Technical report, Universitat des Saarlandes, 2002.

[36] C.F. Westin and S.E. Maier. A dual tensor basis solution to the stejskal-tanner equations for DTMRI. In *Proceedings of International Society for Magnetic Resonance in Medicine*, 2002.

[37] C.F. Westin, S.E. Maier, B. Khiddir, P. Everett, F.A. Jolesz, and R. Kikkinis. Image processing for diffusion tensor magnetic resonance imaging. In *2nd Int. Conf. on medical Image Computing and Computer-Assisted Intervention*, volume 1679 of *LNCS*, pages 441–452. Springer, September 1999.

[38] C.F Westin, S.E Maier, H. Mamata, A. Nabavi, F.A. Jolesz, and R. Kikinis. Processing and visualization for diffusion tensor MRI. In *In proceedings of Medical Image Analysis*, volume 6, pages 93–108, 2002.